GS2025-18

Drone photogrammetry acquisition in support of geological field mapping in recently burnt forested terrain, west-central Manitoba (part of NTS 63K13)

by J. Marks

In Brief:

- Photogrammetry was effective in recently burned forested terrain
- The data was of sufficient quality and detail to aid potential future geological mapping projects
- Contributing to more efficient geological mapping approaches supports resource development and economic growth

Citation:

Marks, J. 2025: Drone photogrammetry acquisition in support of geological field mapping in recently burnt forested terrain, west-central Manitoba (part of NTS 63K13); *in* Report of Activities 2025, Manitoba Business, Mining, Trade and Job Creation, Manitoba Geological Survey, p. 167–173.

Summary

A photogrammetry survey was flown near Flin Flon, west-central Manitoba, to assess its effective-ness for geological field mapping. The objective of this study was to create a repeatable procedure and evaluate its viability for future implementation elsewhere. Recently burnt terrain provided ideal conditions for the photogrammetry survey, as the area was previously covered by a dense vegetation canopy. Two separate flight heights were chosen to assess whether higher resolution data justifies the additional time required to collect it. The 90 m above ground level (agl) dataset provided comparable data to the 50 m agl dataset, and covered approximately 2.8 times more area after normalizing total flight time between the datasets. Furthermore, the 90 m digital terrain model correlates well with previously noted fault and outcrop locations, which are key aspects of geological mapping. A replicable process was created and can be used as an approach for future projects in similar conditions.

Introduction

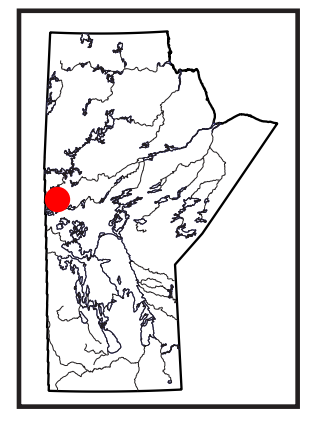
A drone-based photogrammetry survey was conducted by the Manitoba Geological Survey (MGS) to assess the efficacy of using its data to aid geological field mapping efforts. The primary objective was to determine if photogrammetry could provide enhanced, high-quality datasets to aid in geological mapping. Recently burnt forested areas provide ideal conditions for photogrammetric surveys due to the reduction of the ground vegetation and canopy cover, which typically hinders photogrammetric terrain model generation by obstructing the view of the ground surface (Wallace et al., 2016).

The study area, located 15 km east of Flin Flon, was selected for its burnt forest conditions and its potential for future geological field mapping, while also having some pre-existing geological information for comparison purposes (Gale and Babek, 2002). The area was sectioned into two overlapping flight blocks, each with subsequent subblocks to allow for a complete flight within a single battery charge (Figure GS2025-18-1). To assess the trade-off between coverage and data quality, the two flight blocks were flown at different heights; block A at 90 m and block B at 50 m above ground level (agl), which corresponds to a predicted ground sample distance (GSD) of 2.4 and 1.3 cm/pixel, respectively. The methodology was designed to compare the resolutions at different flight heights, measured by GSD, and to determine if the additional time required for higher resolution data collection was justified for geological mapping purposes.

Methodology and survey design

Both blocks were flown with a SZ DJI Technology Co., Ltd. Mavic 3 Enterprise drone, using its wide-angle lens and integrated DJI D-RTK2 real-time kinematic (RTK) system. Utilization of an RTK system eliminated the need for ground control points (GCPs), while still maintaining sufficient positional accuracy (Pugh et al., 2021; Alkan, 2024). Survey parameters were selected to balance flight efficiency and data quality, while ensuring adequate GSD and image overlap. For all flights:

- all images were captured at a nadir orientation (camera angle of 90°);
- overlap was set to 80% frontal and 75% side to ensure sufficient image redundancy and robust 3-D model generation (Lopes Bento et al., 2022);
- azimuth was set to 90° to optimize flight efficiency by flying crosswind to the predominant north-south winds in the area (Chu et al., 2021); and
- terrain-following modes were used to maintain constant flight height agl, which improves overall data accuracy by providing more consistent GSD throughout flights (Singh et al., 2023).



Report of Activities 2025

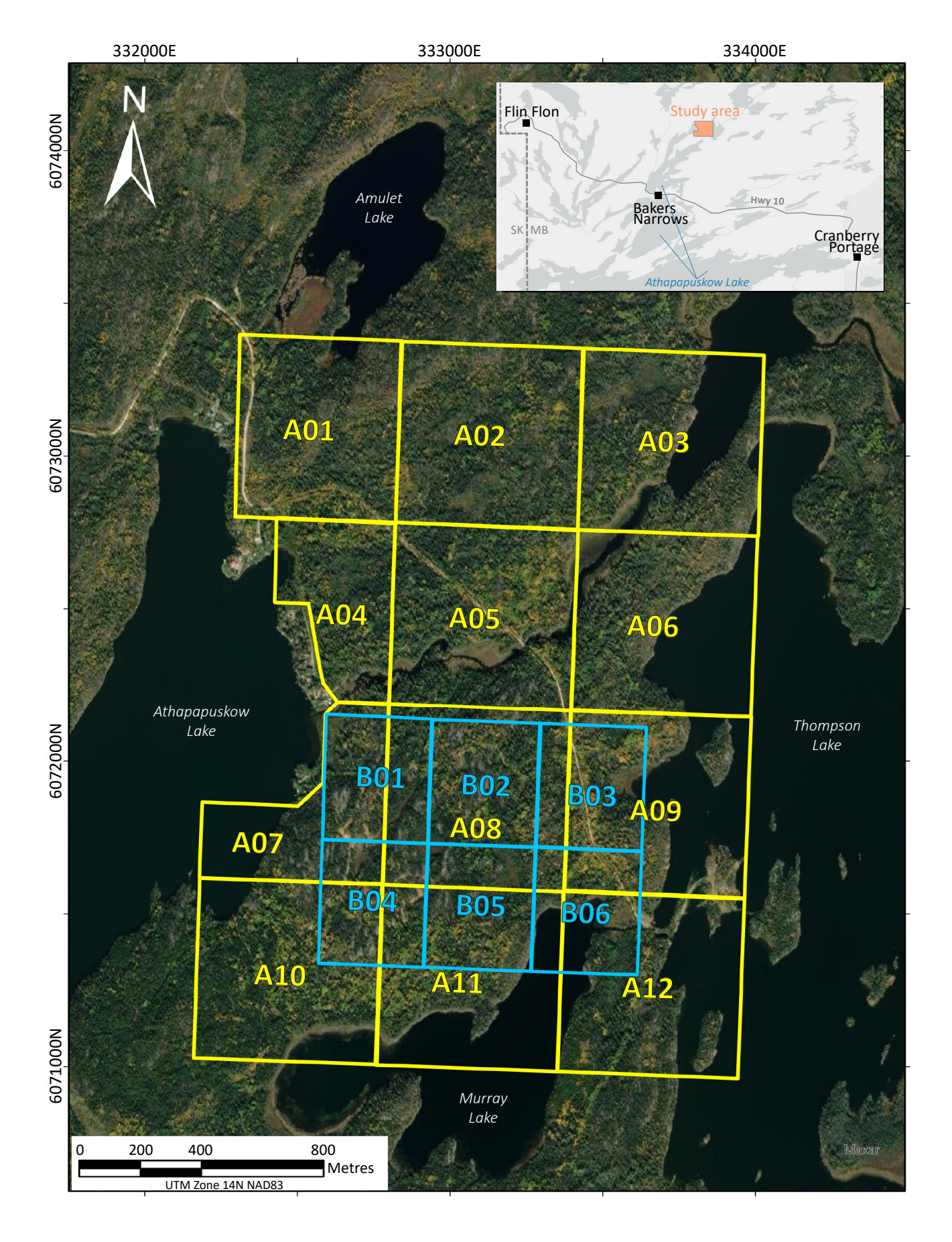


Figure GS2025-18-1: Locations of flight blocks A and B. Blue and yellow polygons indicate outlines of subblocks within each flight block. Inset shows the location of the study area within west-central Manitoba. Satellite imagery from Esri* (2023), © Maxar 2021.

Table GS2025-18-1 shows additional flight parameters used for each survey block. A lower flight height for block B facilitated a slower flight speed to mitigate increased risk of photograph motion blur.

The drone imagery was processed using OpenDroneMap™ WebODM™, an open-source photogrammetry software. Subblocks were processed separately, generating four primary outputs for each:

- 1) orthomosaic
- 2) digital surface model (DSM)
- 3) digital terrain model (DTM)
- 4) 3-D point cloud

Orthomosaic resolution was set to match the GSD and images were not resized prior to processing. The DSM and DTM resolutions were set to 5 cm/pixel. The DTM was created by filtering the DSM using a simple morphological filter (SMF), with the goal of isolating the ground surface by attempting to remove all nonground objects. The DTM datasets were stitched together postprocessing using Esri® ArcGIS® Pro to obtain a combined dataset for each survey block.

Results

The results of the survey showed that block A covered approximately 2.8 times more area than block B after normalizing for total flight time. Both blocks yielded low 3-D root mean square errors (RMSEs) and good position accuracy indicating the collection of high-quality data (Table GS2025-18-2), which is supported by the precise mapping of the road through the study area (black dotted line in Figure GS2025-18-2). Absolute accuracy is not provided as GCPs were not utilized.

Artifacts are present in low-elevation areas within both blocks, contributing to areas of missing data in block A (white areas in Figure GS2025-18-2). These artifacts are due to the presence of water (blue lines in Figure GS2025-18-2), which classically hinders aerial photogrammetric processing (Acharya et al., 2021). Even though most vegetation was removed by the fire, some ground vegetation and canopy cover remained. The SMF filtered most of this vegetation well, but some areas of dense canopy persisted in block A's dataset (black arrows in Figure GS2025-18-2). Additionally, decimetre-scale ground vegetation is present throughout both datasets, however, it does not significantly impact the quality of the data overall.

Table GS2025-18-1: Additional flight parameters for flight blocks A and B. Abbreviations: agl, above ground level; GSD, ground sample distance.

Parameter	Block A	Block B
Flight height (agl)	90	50
Flight speed (m/s)	10	7.5
Estimated line spacing (m)	32	18
Predicted GSD (cm/pixel)	2.4	1.3

Table GS2025-18-2: Parameters resulting from data processing for flight blocks A and B. Abbreviations: CE90, circular error at 90% confidence; GSD, ground sample distance; LE90, linear error at 90% confidence.

Parameter	Block A	Block B
Flight time (h:min)	4:43	2:53
Total area (km²)	4.099	0.909
Average GSD (cm/pixel)	2.325	1.600
3-D root mean square error	0.114	0.058
Relative horizontal accuracy, CE90 (m)	0.098	0.057
Relative vertical accuracy, LE90 (m)	0.183	0.109

A comparison between block A and block B data reveals that block B has a cleaner dataset overall (Figure GS2025-18-3). This is due to its lower GSD and relatively denser point cloud. When comparing the DTMs, block B features appear sharper and ground vegetation is less prevalent (dashed ellipses in Figure GS2025-18-3a, b), resulting in a more accurate ground surface representation. Block B data also provided slightly higher resolution orthomosaics (Figure GS2025-18-3c, d).

Despite these differences, the datasets are quite similar at this scale. All significant topographical features visible in block B are also present in block A, suggesting that no significant information is gained from the former (Figure GS2025-18-3a–d). These similarities are likely related to the smaller difference between the calculated GSDs of the two datasets (Table GS2025-18-2), than in their predicted GSDs (Table GS2025-18-1), as GSD is a direct measurement of spatial resolution. Variations between predicted and calculated GSDs are generally caused by unexpected variations in flight height (Kozmus Trajkovski et al., 2020).

Discussion

The DTM produced for block A provides an accurate representation of the topography in the study area. Such models can provide a valuable resource for identifying geomorphological or structural features. For example, DTM data show a distinct northeast-southwest topographical trend in block A (Figure GS2025-18-2). This correlates well with mapped outcrops (Gale and Babek, 2002), which are associated with local elevation highs and show a similar directional trend (black outlined polygons in Figure GS2025-18-4). Another example is the presence of a prominent northeast-trending lineation in the northeastern portion of block A, which strongly correlates to a structural fault interpreted by Gale and Babek (2002; Figures GS2025-18-2, -4). Features such as these become clearly visible in high-resolution DTM data, which can be more difficult to identify with traditional methods, and can help provide a foundation for detailed geological mapping.

This study also highlighted the critical role of site selection for photogrammetry. Some areas of surviving canopy cover were not removed by the SMF due to their size and density (Figures GS2025-18-2, -3a, b), demonstrating the challenge that photogrammetric processing has when trying to accurately

Report of Activities 2025

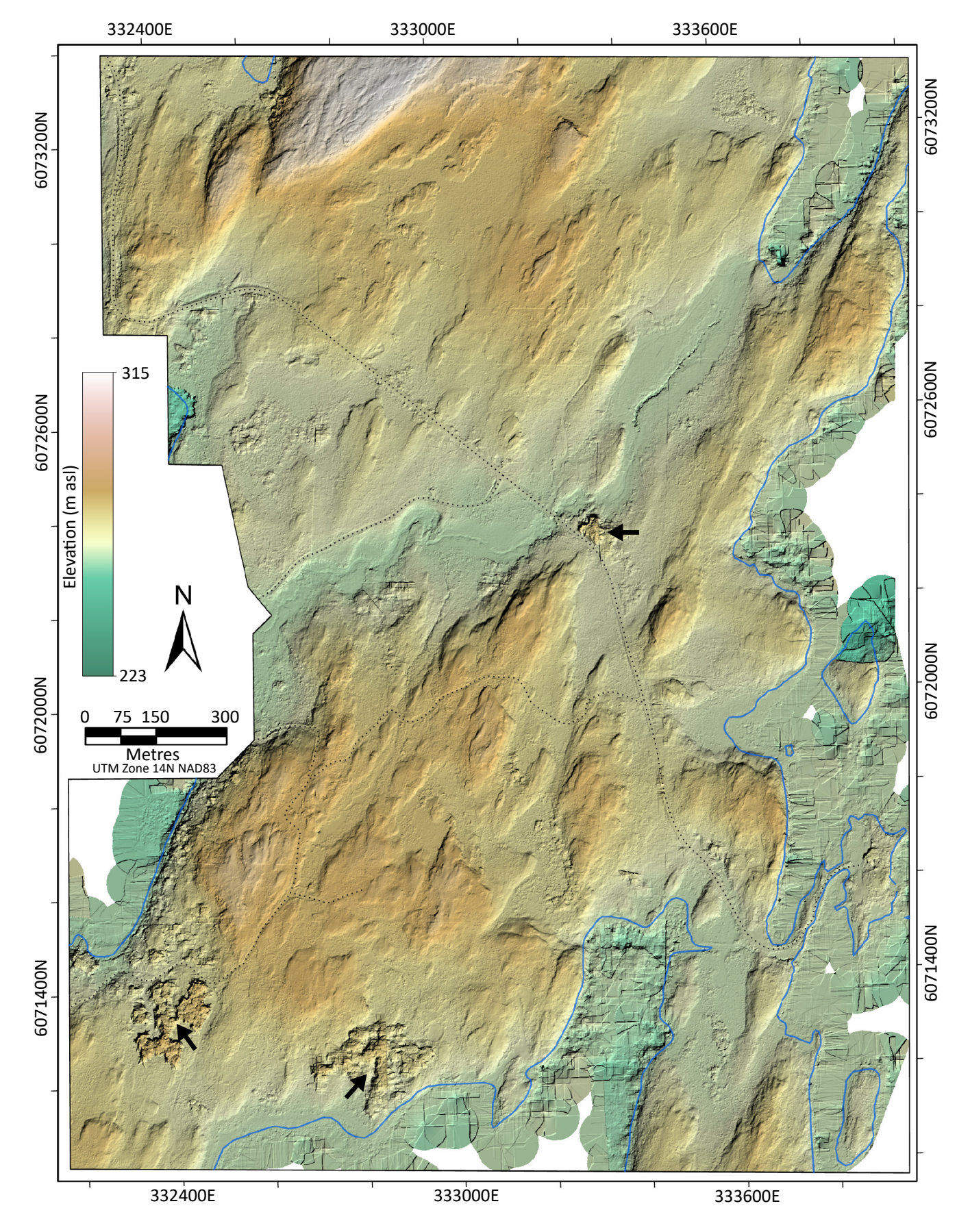


Figure GS2025-18-2: Results showing digital terrain model (DTM) for flight block A in shaded relief. Dotted lines highlight roads distinguishable within the DTM data. Black arrows indicate areas of vegetation that persisted through simple morphological filtering. Blue lines outline approximate water body boundaries (from Gale and Babek, 2002). White areas represent areas of missing data.

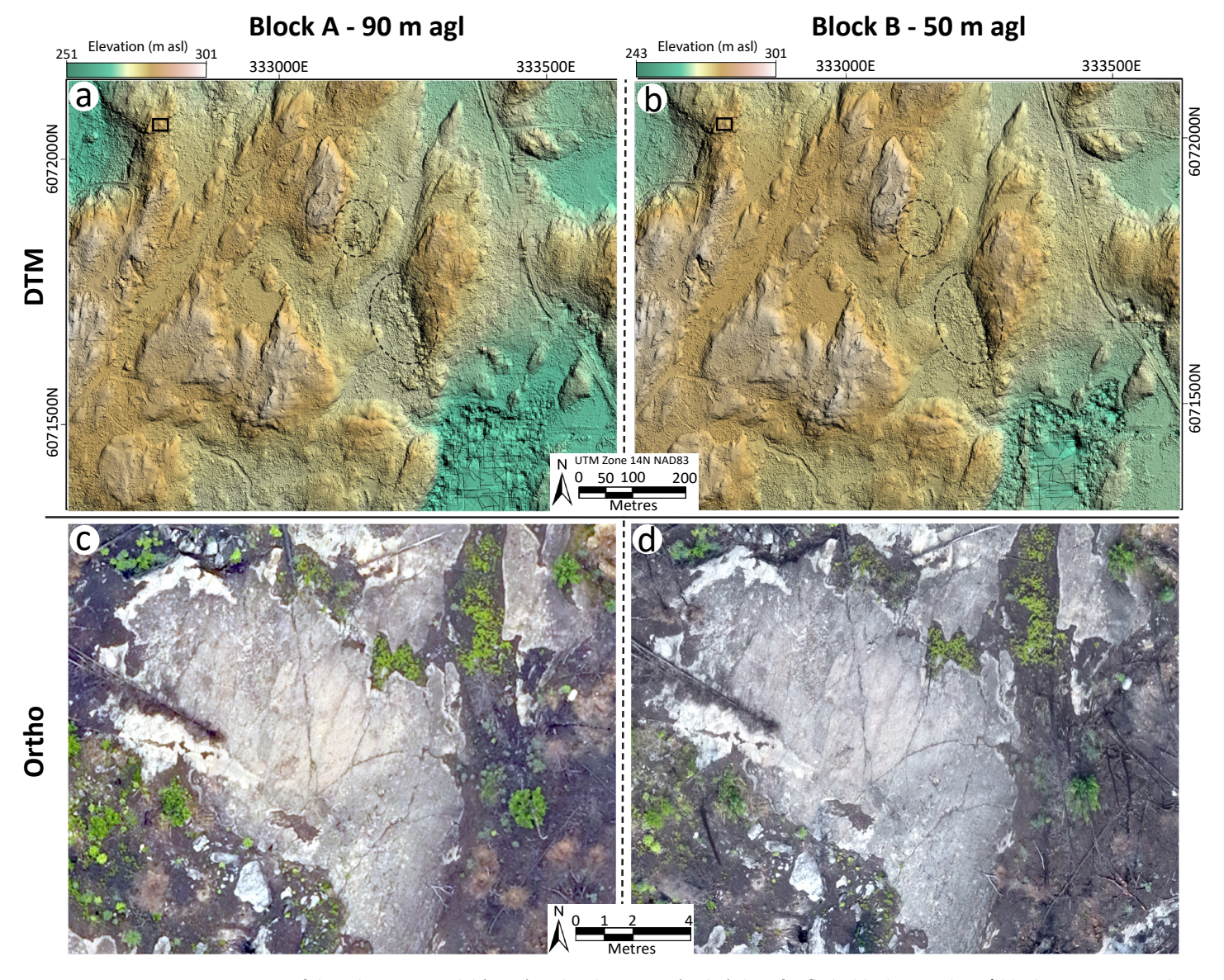


Figure GS2025-18-3: Comparison of digital terrain model (DTM) and orthomosaic (ortho) data for flight blocks A and B: a) block A DTM, 90 m above ground level (agl); b) block B DTM, 50 m agl; c) block A orthomosaic, 90 m agl; d) block B orthomosaic, 50 m agl. Dashed ellipses in a) show locations of vegetation within block A that persisted after filtering. Dashed ellipses in b) show the vegetation was filtered out in block B. Black square in a) and b) indicates the location within the DTM of the orthomosaics in c) and d).

model the ground surface. These challenges can be mitigated by increasing image overlap or performing additional flights at different heights and camera angles, thus increasing the chance of generating ground points beneath the canopy surface (Pessacg et al., 2022). However, these methods would significantly decrease data collection efficiency, and increase time required for processing. This reinforces the value of conducting this study in recently burnt forested terrain, as it allowed for the efficient production of high-quality data by minimizing the challenges typically associated with photogrammetry in forested terrain.

Economic considerations

Geological mapping is a vital tool with many applications. For Manitoba, it plays a fundamental role for informing land-use

decisions, understanding geological features and the tectonic evolution of terrains through time, and assessing the economic potential of a region. Geological mapping is also used by the exploration and mining industry, providing critical data for resource exploration and economic planning. Increased forest fire activity this past summer provided potential target areas for photogrammetry surveys in terrain that is now better exposed. These surveys can offer rapid and effective means to acquire data to aid geological field mapping. Acquiring these types of data is particularly relevant given the increasing global demand for critical minerals and Manitoba's critical minerals strategy, which highlights the need for accelerated geological investigations to support resource development and economic growth. The successful application of this survey framework provides a replica-

Report of Activities 2025 171

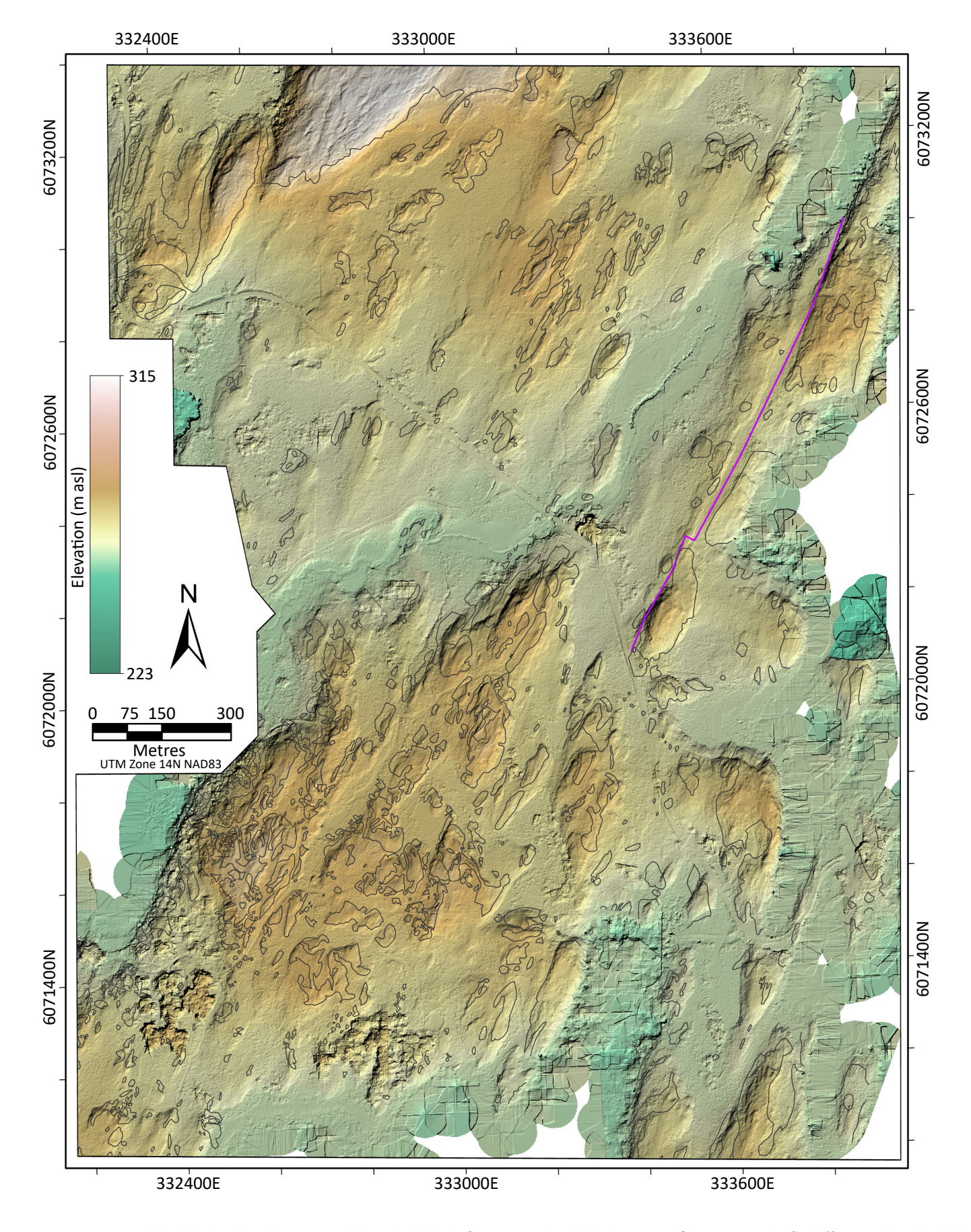


Figure GS2025-18-4: Flight block A digital terrain model in shaded relief, annotated with the locations of outcrops and a fault (from Gale and Babek, 2002). Black polygons outline outcrop locations. Purple line shows location of an interpreted fault.

ble approach for future projects, contributing to more efficient approaches to geological mapping.

Acknowledgments

The author acknowledges K.D. Reid from the Manitoba Geological Survey for his geological insights and his part in generating the project. D. Koop is thanked for graciously providing accommodations during the fieldwork, and W. Sharpe (summer student, University of Manitoba) is thanked for his assistance with data collection. Lastly, C. Epp, E. Ralph and P. Belanger (Manitoba Geological Survey) are thanked for their roles in equipment expediting and maintenance.

References

- Acharya, B.S., Bhandari, M., Bandini, F., Pizarro, A., Perks, M., Joshi, D.R., Wang, S., Dogwiler, T., Ray, R.L., Kharel, G. and Sharma, S. 2021: Unmanned aerial vehicles in hydrology and water management: applications, challenges, and perspectives; Water Resources Research, v. 57, no. 11, art. e2021WR029925.
- Alkan, M.N. 2024: High-precision UAV photogrammetry with RTK GNSS: eliminating ground control points; Hittite Journal of Science and Engineering, v. 11, no. 4, p. 139–147.
- Chu, T., Starek, M.J., Berryhill, J., Quiroga, C. and Pashaei, M. 2021: Simulation and characterization of wind impacts on sUAS flight performance for crash scene reconstruction; Drones, v. 5, no. 3, art. 67.
- Esri® 2023: World imagery map, April 05, 2021; Esri, no scale given, URL https://services.arcgisonline.com/ArcGIS/rest/services/World_Imagery/MapServer [September 2025].

- Gale, G.H. and Babek, L.B. 2002: Geology of the Baker Patton Complex, Flin Flon, Manitoba (parts of NTS areas 63K 12, 13); Manitoba Industry, Trade and Mines, Manitoba Geological Survey, Geoscientific Map MAP2002-1, scale 1:10 000.
- Kozmus Trajkovski, K., Grigillo, D. and Petrovič, D. 2020: Optimization of UAV flight missions in steep terrain; Remote Sensing, v. 12, no. 8, art. 1293.
- Lopes Bento, N., Araújo E Silva Ferraz, G., Alexandre Pena Barata, R., Santos Santana, L., Diennevan Souza Barbosa, B., Conti, L., Becciolini, V. and Rossi, G. 2022: Overlap influence in images obtained by an unmanned aerial vehicle on a digital terrain model of altimetric precision; European Journal of Remote Sensing, v. 55, no. 1, art. 2054028.
- Pessacg, F., Gómez-Fernández, F., Nitsche, M., Chamo, N., Torrella, S., Ginzburg, R. and De Cristóforis, P. 2022: Simplifying UAV-based photogrammetry in forestry: how to generate accurate digital terrain model and assess flight mission settings; Forests, v. 13, no. 2, art. 173.
- Pugh, N.A., Thorp, K.R., Gonzalez, E.M., Elshikha, D.E.M. and Pauli, D. 2021: Comparison of image georeferencing strategies for agricultural applications of small unoccupied aircraft systems; The Plant Phenome Journal, v. 4, no. 1, art. e20026.
- Singh, C.H., Mishra, V. and Jain, K. 2023: High-resolution mapping of forested hills using real-time UAV terrain following; ISPRS Annals of the Photogrammetry, Remote Sensing and Spatial Information Sciences, v. X-1/W1-2023, p. 665–671.
- Wallace, L., Lucieer, A., Malenovský, Z., Turner, D. and Vopěnka, P. 2016: Assessment of forest structure using two UAV techniques: a comparison of airborne laser scanning and structure from motion (SfM) point clouds; Forests, v. 7, no. 3, art. 62.

Report of Activities 2025 173